ACS Medicinal Chemistry Letters

pubs.acs.org/acsmedchemlett Letter

Overcoming the Pregnane X Receptor Liability: Rational Design to Eliminate PXR-Mediated CYP Induction

Joshi M. Ramanjulu,* Shawn P. Williams, Ami S. Lakdawala, Michael P. DeMartino, Yunfeng Lan, and Robert W. Marquis

Cite This: https://doi.org/10.1021/acsmedchemlett.1c00187 Read Online

ACCESS | Metrics & More | Article Recommendations | Supporting Information

ABSTRACT: The pregnane X receptor (PXR) regulates expression of proteins responsible for all three phases required for the detoxification mechanism, which include CYP450 enzymes, phase II enzymes, and multidrug efflux pumps. Therefore, PXR is a prominent receptor that is responsible for xenobiotic excretion and drug−drug interactions. Pyrimidinone **1** is an antagonist of the calcium sensing receptor (CaSR) and a strong activator of PXR. Repeat oral administration revealed diminished exposures over time, which prohibited further progression. A medicinal chemistry campaign was initiated to understand and abolish activation of PXR in order to increase systemic exposures. Rational structure−activity relationship investigations utilizing cocrystal structures and a de novo pharmacophore model resulted in compounds devoid of PXR activation. These studies culminated in the first orally active CaSR antagonist **8** suitable for progression. Cocrystallography, the pharmacophore model employed, and additional observations reported herein supported rational elimination of PXR activation and have applicability across diverse chemical classes to help erase PXR-driven drug−drug interactions.

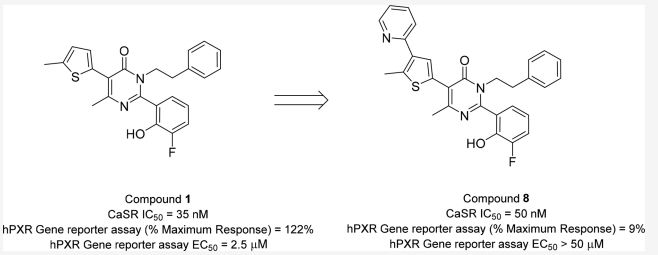

KEYWORDS: *Pregnane X receptor, drug−drug interactions, CYP induction, calcium sensing receptor, parathyroid hormone, pyrimidinone, pharmacophore model*

The family of cytochrome P450 (CYP) enzymes play an integral role in drug−drug interactions because of their efficient yet promiscuous metabolizing capabilities. Among CYP isoforms, CYP3A4 is known to metabolize greater than 50% of marketed drugs. The induction of CYP3A has been heavily investigated in preclinical drug discovery and human trials.[1] Pregnane xenobiotic receptor (PXR) has garnered much attention because it plays a major role in the induction of CYP3A, leading to drug−drug interactions (DDIs).[2] PXR belongs to the nuclear receptor (NR) superfamily and is mainly expressed in the liver, intestine, and colon, where most drug-metabolizing enzymes are also expressed and regulated. PXR is a multidomain protein with two key domains, a highly conserved DNA-binding domain (DBD) and the largest, moderately conserved ligand-binding domain (LBD).[3] Substantial divergence in recognition of small molecules is noted among species as a result of the low sequence conservation of the LBD. For example, the LBD shares amino acid identities of only 76% between human and rodent species and significantly less for lower-order species (∼50%).[4−7] Upon activation, PXR transcriptionally induces genes that express proteins known to play key roles in all three phases of metabolism−excretion mechanisms: (a) CYP enzymes, including CYP3A4; (b) conjugation enzymes, including carboxylesterases; and (c) transporters such as MDR1.[8,9] Thus, PXR-mediated clearance is highly evolved to regulate an entire network of genes that are involved in the metabolism and excretion of endo- and xenobiotics from the body (Figure 1).[10,11]

Crystal structures of the human PXR LBD apo- and ligand-bound complexes were first reported in 2001.[12] Subsequently, several other cocrystal structures have been reported.[13] The PXR LBD binding pocket is extremely large, flexible, and hydrophobic in nature. The cavity is lined with 28−30 amino acid residues, among which only six are polar residues, and these are evenly distributed throughout the surface of the largely hydrophobic cavity. The volume of the apo binding pocket is ∼1250 Å^3 and has been shown to expand to ∼1544 Å^3 to accommodate molecules of various sizes (≤230 to >800 Da). Despite the presence of hydrophobic residues, this pocket is capable of binding polar molecules (cLogP > 1) and yet flexible enough to bind to hydrophobic molecules (cLogP = 8). The initial crystal structures reported by Watkins et al.[12] demonstrated a single ligand existing in multiple binding

Received: April 2, 2021
Accepted: August 2, 2021

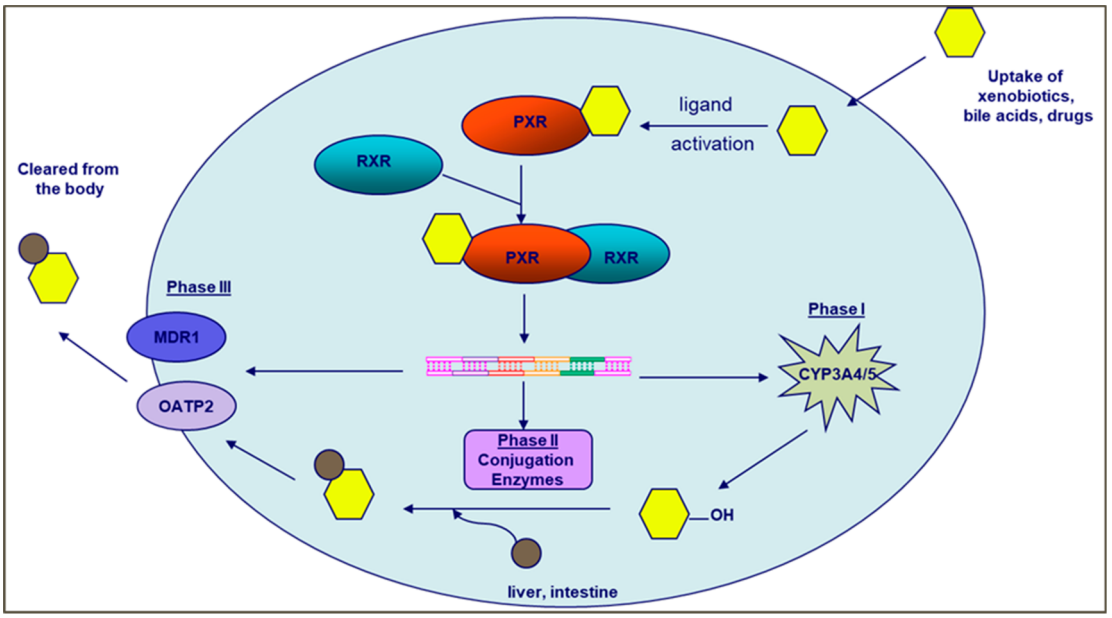

Figure 1. Role of PXR in the regulation of xenobiotic metabolism.

Table 1. Mouse Toxicokinetic Parameters (Composite Sampling) for Compound 1

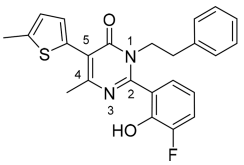

Compound **1**
CaSR IC_{50} = 51 nM
hPXR Gene reporter assay (% Maximum Response) = 122%
hPXR Gene reporter assay EC_{50} = 2.5 μM
CYP3A4 - Induction h-Hepatocyte (% Maximum Response) = 10, 54, 42

	AUC_{0-t} (μg h/mL)			C_{max} (μg/mL)		
dose (mg kg^{-1} day^{-1})	day 1	day 10	fold diff.	day 1	day 10	fold diff.
300	2.88	1.26	−2.28	0.98	0.82	−1.2
1000	10.8	2.85	−3.79	2.96	0.68	−4.4
2000	15.1	1.58	−9.56	3.60	0.48	−7.5

orientations. Inspection of subsequent cocrystal structures revealed different amino acid residues engaging ligands from diverse structural classes, increasing the difficulty of predicting the key interactions required for affinity and activation.[14] In silico models developed previously to guide structure−activity relationship (SAR) investigations were deemed unreliable given the promiscuous nature of the binding cavity coupled with the possibility of multiple binding orientations.[15,16] In balancing the learnings from these articles with advantages and disadvantages of 3D−5D QSAR and docking models, we have pursued a combination of methods relying on internal and external crystal structures to develop a pharmacophore model to guide docking algorithms.

The calcium sensing receptor (CaSR) located on the parathyroid gland functions as the principal regulator of parathyroid hormone (PTH) secretion.[17] PTH(1−84) has been clinically validated as a bone-forming agent and used to treat osteoporosis in both its truncated (Forteo) and full-length (Preos) forms.[17] Both forms of approved PTH therapies require daily injections. An alternative therapeutic approach would be to use orally bioavailable small-molecule antagonists of the CaSR to stimulate secretion of endogenous PTH, thus making them potential treatments for osteoporosis. One such CaSR antagonist, compound **1**, was identified as suitable for progression into rodent toxicology studies. Oral administration of compound **1** in mice at 300, 1000, and 2000 mg kg^{-1} day^{-1} for 10 days resulted in significantly diminished exposures (both area under the curve (AUC) and maximum concentration (C_{max})) on day 10 compared with day 1. The reduction in exposure was dose-dependent, with about 2-, 4-, and 10-fold drops at 300, 1000, and 2000 mg/kg, respectively (Table 1). Compound **1** is a substrate for CYP3A4 and was therefore presumed to be eliminated via phase I metabolism.[18] As this mechanism was unable to explain the larger drop at higher doses, it was hypothesized that the compound may induce higher levels of the CYP3A4 enzyme upon repeated treatment, thus leading to diminishing exposure over the course of the study. With this in mind, compound **1** was evaluated in a PXR functional assay, which confirmed the induction potential for CYP3A4. This result was further validated in a human hepatocyte induction assay that has a strong clinical correlation with drugs that elicit PXR-mediated CYP3A4 induction.[19,20] Further evaluation of compound **1** in a binding assay confirmed its affinity toward human PXR (hPXR) and demonstrated greater induction potential in mouse and human compared with rat PXR assays (pp S7, S17 and S18 in the Supporting Information (SI)). Finally, other members from this class of pyrimidinones also exhibited high affinity for hPXR, thus confirming the observations from the toxicology

https://doi.org/10.1021/acsmedchemlett.1c00187
ACS Med. Chem. Lett. XXXX, XXX, XXX−XXX

Scheme 1. Synthesis of 2-(3-Fluoro-2-hydroxyphenyl)-6-methyl-5-(5-methylthien-2-yl)-3-(2-phenylethyl)-4(3*H*)-pyrimidinone (1)[a]

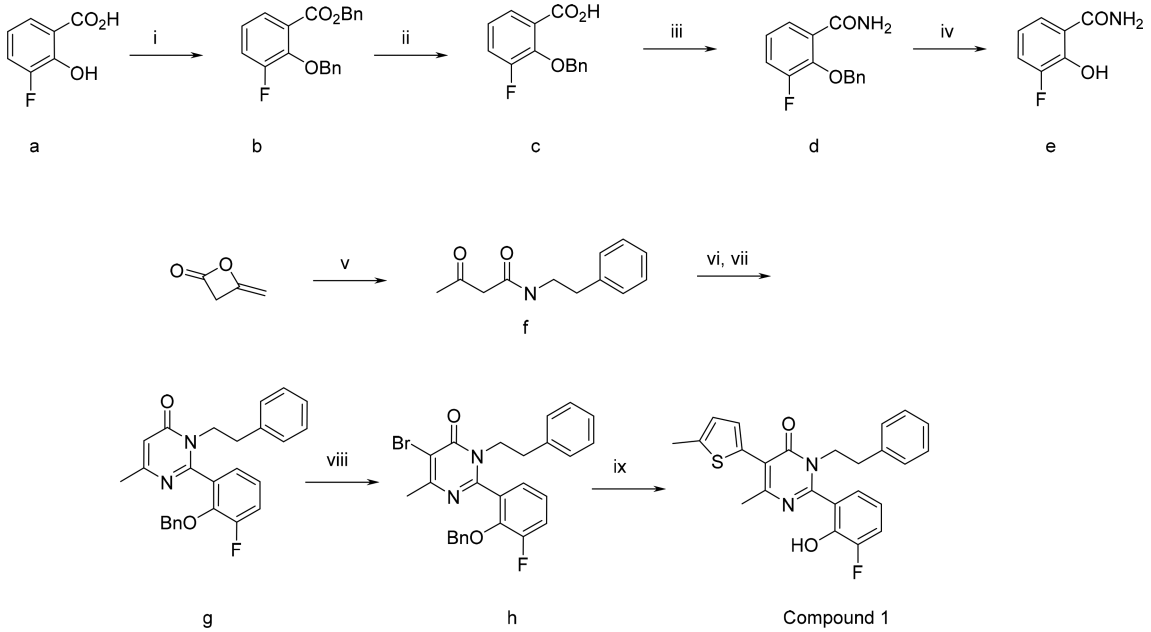

[a]Reagents and conditions: (i) benzyl bromide, K_2CO_3, DMF; (ii) NaOH, MeOH, H_2O; (iii) ethyl chloroformate, TEA, THF, NH_4OH; (iv) 10% Pd/C, 40 psi, EtOH; (v) phenethylamine, Et_2O, reflux; (vi) Ti(*i*PrO)$_4$, **e**, reflux; (vii) benzyl bromide, K_2CO_3, DMF; (viii) Br_2, AcOH; (ix) $Pd(PPh_3)_4$, EtOH, H_2O, Na_2CO_3, 5-methylthiophene-2-boronic acid, microwave.

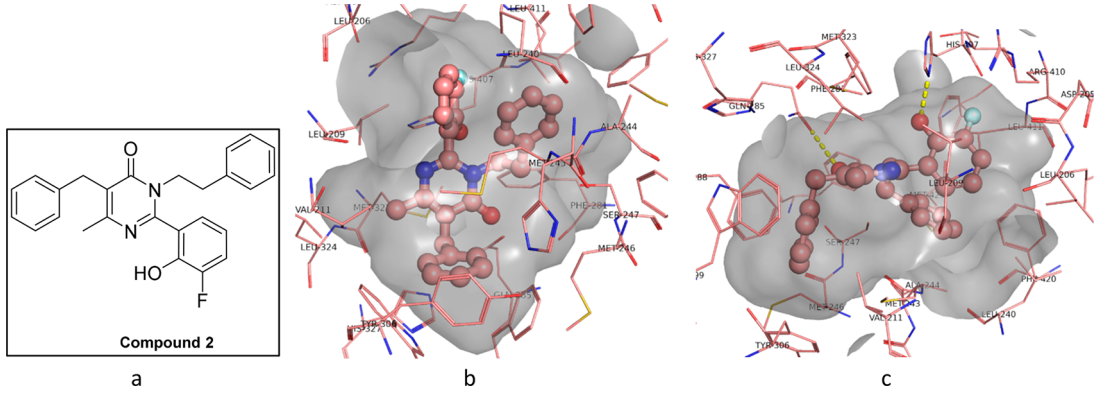

Figure 2. (a) Structure of compound **2**. (b, c) Cocrystal structures showing pocket residues in contact with and in proximity to the bound ligand.

study and the induction potential of the pyrimidinone class of compounds.

To explore and expedite the SAR to overcome PXR induction, several synthetic methodologies were applied (Scheme 1).[21−24] The synthesis of compound **1** began with 3-fluoro-2-hydroxybenzoic acid, which was reacted with benzyl bromide followed by hydrolysis to provide carboxylic acid **c**. Carboxylic acid **c** was then converted to the amide using the mixed anhydride, and treatment with ammonium hydroxide followed by benzyl deprotection provided the intermediate 3-fluoro-2-hydroxybenzamide (**e**). The second key intermediate, 3-oxo-*N*-(2-phenylethyl)butanamide (**f**), was prepared by refluxing diketene in anhydrous ether with phenethylamine. Next, the reaction of intermediates **e** and **f** in refluxing titanium isopropoxide, a novel synthetic methodology developed at GSK,[23] furnished the pyrimidinone scaffold in one step, and subsequent benzyl protection produced pyrimidinone **g**. Selective bromination at C5 under acidic conditions followed by $Pd(PPh_3)_4$-catalyzed Suzuki reaction under microwave conditions with 5-methylthiophene-2-boronic acid furnished compound **1**.

As discussed earlier, published pharmacophore models generated from computational methods proved to be unreliable to identify residues critical for PXR induction.[14−16] Additionally, the possible existence of multiple binding modes also complicates the development of in silico models to aid SAR investigations. To date, no pharmacophore model has been successfully applied to eliminate PXR-mediated induction of CYP3A4. With this in mind, we initiated cocrystallization trials for pyrimidinone-based agonists of PXR that were highly active in the functional assay (% maximum response > 70% and EC_{50} < 3 μM). Several pyrimidinone-based compounds resulted in cocrystal structures at a resolution of 2.25−3.00 Å. To our delight, all of the crystal structures unambiguously revealed a single binding mode (Figure 2). The C2 aromatic moiety (2-fluorophenol) is twisted out of the plane to engage with His407 via a hydrogen bond (H-bond) interaction. Gln285 is involved in a second H-bond interaction with the

https://doi.org/10.1021/acsmedchemlett.1c00187
ACS Med. Chem. Lett. XXXX, XXX, XXX−XXX

carbonyl group of the pyrimidinone scaffold. Both His407 and Gln285 are involved in H-bond interactions, as previously reported by several groups.[14] Taken together, these results indicate that these two residues play a prominent role via "anchoring" and "aligning" small molecules, thereby facilitating subsequent high-affinity hydrophobic interactions. The anchored pyrimidinone projects the C5 benzyl group into the highly hydrophobic bottom pocket that is shaped by Phe281, Phe288, Trp299, and Tyr306. In this orientation, the C5 benzyl group engages in a face-to-face $\pi-\pi$ stacking interaction with Trp299 and edge-to-face interactions with Phe288 and Tyr306 at distances ranging from 3.67 to 4.40 Å. The N3 phenethyl substituent nestles into the hydrophobic back pocket that is encapsulated by Leu240, Ile414, and Phe420. The extended phenyl group is engaged in edge-to-face $\pi-\pi$ stacking with Phe420. The contribution of hydrophobicity to the drug−receptor complex is more energetically favorable than polar interactions. Thus, the collective contributions of the above hydrophobic interactions lead to the tight binding nature of pyrimidinone-based CaSR analogues to the LBD of PXR.

The ligand-binding pocket located in the LBD is predominately hydrophobic in nature and is lined by 28 amino acid residues that are desolvated when bound to compound **2** (Figure 2). Comparison of the apo and ligand-bound structures revealed only minor changes with a root-mean-square deviation of 0.242 Å over all atoms in the 28 residues. The cavity volume is 1289 $Å^3$, which is 29 $Å^3$ larger than that of the apo structure but only 5 $Å^3$ smaller than the pocket in the SR12813 complex[25,26] and many of the reported structures.[12,13] Four polar residues (Gln285, His407, Arg410, and Ser208) are situated at the peripheral portion of the cavity, while hydrophobic groups are lined up in the inside. The two critical polar groups (Gln285 and His407) extend out into the middle of this pocket to anchor small molecules that can engage such interactions.

Our data demonstrating a single binding mode are at odds with an earlier hypothesis that cocrystallization methods in the absence of the coactivator SRC-1 likely result in multiple binding modes.[13] SRC-1 binds to the activation factor 2 region within the LBD and is thought to be involved in rigidifying the binding pocket, thus limiting multiple orientations. To gather further evidence to support the observed single binding mode, cocrystallization of additional analogues was pursued using identical crystallization methods. The results indicated that, similar to the structures with compound **2**, a single binding mode was present for each analogue examined (compounds **9** and **10**; SI p S10), and the orientations and conformations of all three compounds within the pocket are similar. Furthermore, all of the residues surrounding the binding cavity remain fixed except for Leu209 (Figure 2). The key H-bonds with His407 and Gln285 are maintained with the C5 moiety projected into the hydrophobic cavity at the bottom of the pocket (Figure 3). A possible explanation for the existence of only one conformation is that the contribution from the H-bond interactions and hydrophobic interactions is significantly higher for pyrimidinones relative to other binders, thus limiting the motion within the binding pocket. In contrast, the H-bond donor (phenol moiety) and corresponding polar interaction for SR12813 (Table S1) are significantly weakened by the presence of two ortho *tert*-butyl groups, leading to existence of multiple binding conformations.

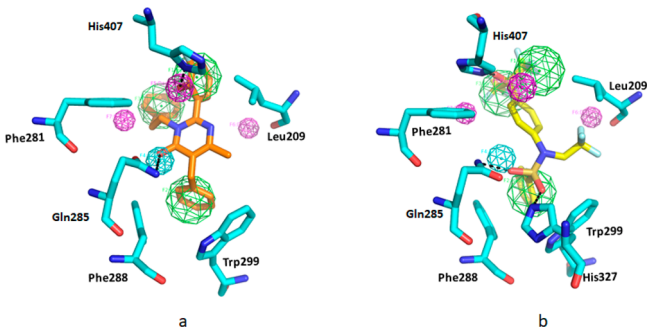

Figure 3. (a) Structure of compound **2** anchored via the two polar residues His407 and Gln285, with the benzyl group sandwiched by Phe288 and Thr299. (b) Structure of T0901317 displaying H-bond interactions of the sulfonyl group with Gln285 and His407 and interactions of the phenyl group with Phe281 and Leu209.

Armed with robust structural biology and institutional knowledge, we built a pharmacophore model in order to rationally design out PXR affinity associated with the pyrimidinone class of CaSR antagonists and for wider applicability. Upon examination of several cocrystal structures, both in-house and published, we selected 10 structures based on molecular properties and bound conformations (Table S1). In particular, both crystal structures of SR12813 were included to dissect the multiconformational binding potential of the LDB.[12] Striking properties of the LBD include the large and flexible binding site, movement of a flexible loop containing residues 309−321 (which allows expansion of the cavity), and binding of compounds with diverse molecular properties. The binding site cavity is composed of 20 hydrophobic, four polar, and four charged residues. We have identified five key polar residues, namely, Ser208, Ser247, Gln285, His407, and Arg410, that are spread across the top of the binding site to form significant interactions with bound ligands. The crystal structures were critically analyzed for ligand binding modes and H-bond and hydrophobic interactions. H-bond interactions were further scrutinized for donor and acceptor characteristics as well as bond strength related to distance and angle. Hydrophobic interactions were inspected similarly and classified as aliphatic versus aromatic, with aromatic contacts further distinguished into face-to-face and edge-to-face interactions. All compounds evaluated had at least two hydrophobic interactions and one H-bond interaction. The pharmacophoric features of each ligand were calculated using Molecular Operating Environment (MOE) and compared to those of other molecules generated with SRC-1 cofactor (SI pp S4 and S11). The resulting 3D pharmacophore features were overlaid, and an overall "average" model was identified (Figure 4). In general, the pharmacophore model has four residues dispersed in the cavity to anchor molecules in the center via H-bond and/or charged interactions. Among the four residues, Leu209 always engaged the molecules via the carbonyl group and contributed to a wider array of molecules compared with Ser247. Gln285 and His407 are the key polar residues, and one of them engaged in H-bonds in all of the cocrystal structures evaluated to date. Hydrophobic residues form the overall "triangular" shape of the cavity, with seven residues concentrated at the three corners. The top left corner is occupied by Met243, while the top right corner contains Leu207 and Leu411, which are hydrophobic in nature but not optimal for engaging aryl groups. The lower portion of the

https://doi.org/10.1021/acsmedchemlett.1c00187
ACS Med. Chem. Lett. XXXX, XXX, XXX−XXX

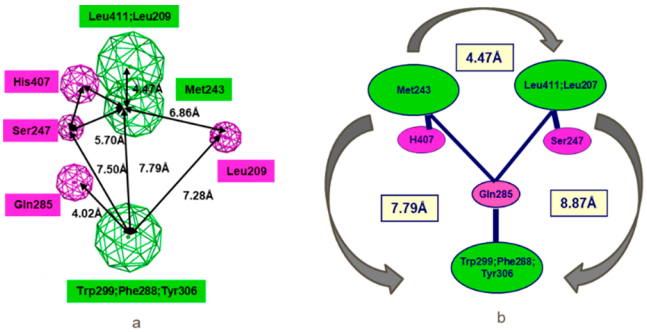

Figure 4. (a) Pharmacophore model displaying key residues engaged binding to a diverse group of compounds. Purple and green spheres represent H-bond and hydrophobic interactions, respectively, while the size of each sphere reflects number of compounds. Distances captured between residues/spaces are depicted. (b) Average distances between the three key groups of hydrophobic residues.

pocket has significant hydrophobic character, is rigid, and is surrounded by three aromatic residues (Phe288, Trp299, and Tyr306). This area accommodates aliphatic and aryl groups and is capable of interacting with aryls in both a face-to-face and edge-to-face manner.

The pharmacophore model triggered a structure-guided investigation to overcome the PXR affinity associated with the pyrimidinone class of CaSR antagonists. As described above, all of the crystal structures of the pyrimidinone analogues demonstrated a single bound conformation. Docking of compound **1** resulted in a similar conformation with the C5 substituent extended into the bottom hydrophobic cavity while anchored to Gln285 via the carbonyl group. The second H-bond is observed to involve the hydroxy group of the C2 aryl group, while the N3 phenethyl group projects out to the back in the pocket without any significant interactions. Overlay of the docked and crystal structures of compound **2** (Figure 5)

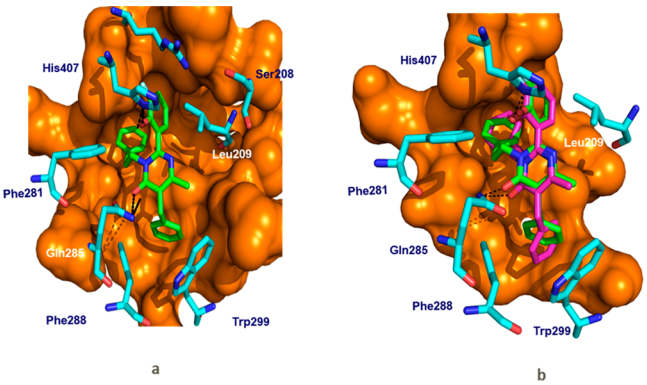

Figure 5. (a) Cocrystal structure of compound **2** depicting key interactions. (b) Docked structure of compound **2**. Both the docked and crystal structures show the critical H-bonds between compound **2** and residues Gln285 and His407.

enhances our confidence that like other cocrystallized pyrimidinones, it exists in the conformation observed experimentally and validates our use of the docking model to drive SAR investigations.

Using information derived from the cocrystal structures and subsequent docking studies, an SAR strategy was employed with the intention of examining the five key interactions observed (Figure 6). All of the new analogues prepared were assessed simultaneously for their CaSR antagonist activity (SI p S5) and in the PXR gene reporter assay (Figure 7and SI pp S7, S8, S17, and S18). The first set of analogues probed the back pocket (N3 substituents); however, these displayed reduced affinity toward PXR and suffered from poor activity against CaSR. The 2-position of the pyrimidinone is the most sensitive, and structural changes are not well-tolerated with respect to CaSR activity. Incorporation of polar heterocycles (compound **5**) dramatically lowered the PXR affinity despite maintaining the key H-bond to His407, suggesting that hydrophobic interactions significantly boost the affinity toward PXR. We then examined the contributions of the H-bond interactions between Gln285 and the carbonyl of the pyrimidinone template. Replacement of the pyrimidinone with pyrazine **3**, which is not capable of engaging in the H-bond interaction with Gln285, demonstrated high levels of PXR affinity, perhaps due to the anchoring H-bond interaction with His407 via 2-hydroxy-3-fluorophenyl moiety at C2. This corroborates our hypothesis that one H-bond interaction is sufficient to anchor small molecules to facilitate secondary hydrophobic interactions as suggested by our analysis.

As detailed earlier, the crystal structure and the docking confirmed that the substituent at C5 of the pyrimidinone template projects out into the bottom "rigid" hydrophobic cavity. To ensure the predominately hydrophobic nature of this pocket area, hydroxymethylthiophene analogue **4** and thiazole analogue **5** were evaluated and, as anticipated, produced dramatic reductions in PXR affinity (Figure 7). Incorporation of a rigid 5-phenylthien-2-yl moiety at C5 of the pyrimidinone resulted in loss of affinity, suggesting a severe steric clash with Trp299. Even though compound **6** is capable of $\pi-\pi$ stacking and/or edge-to-face interactions with either Phe288 or Trp299, this portion of the binding pocket is not flexible enough to accommodate larger groups. This agrees with an earlier report that flexibility was seen only within the three regions that are located at the top of the cavity (200−209, 229−235, and 310−317) but not at the bottom portion of the cavity.[27] On this basis, incorporation of rigid and polar groups would likely produce the optimal profile. In fact, incorporation of polarity through a 5-(pyridin-2-yl)thien-2-yl (**7**) and 4-(pyridin-2-yl)-5-methylthien-2-yl group (**8**) at C5 resulted in dramatic losses in PXR affinity while retaining activity against the CaSR receptor (Figure 7 and SI p S18). Docking clearly indicated that stereoelectronic repulsive forces of the C5 substituent overcame several detrimental interactions (Figure 6). Compound **8** demonstrated a clean profile in the gene reporter assay as well as in the industry-standard human hepatocyte assay. Gratifyingly, assessment of compound **8** in a 10 day repeat dose rat toxicology study demonstrated no PXR-mediated reduction in exposures from day 1 to day 10 at 10-fold higher systemic exposure (Table 2). In comparison, compound **1** had decreased exposure (0.72× in AUC) at day 10 while the compound **8** exposure increased (29.5 vs 41.1 μg h/mL) over the course of the study. As observed in the mouse toxicology study (Table 1), compound **1** induced rodent PXR activation at much lower concentrations, leading to diminished exposure, while with compound **8**, even at >20-fold higher levels (C_{max}), AUC exposure increased 1.4-fold on day 10.

In order to understand whether any general trends related to physicochemical properties were present, we evaluated a much broader data set from the GSK compound collection. Evaluation of PXR activity data from >15 000 compounds provided a few general trends. Molecules that are hydrophobic,

https://doi.org/10.1021/acsmedchemlett.1c00187
ACS Med. Chem. Lett. XXXX, XXX, XXX−XXX

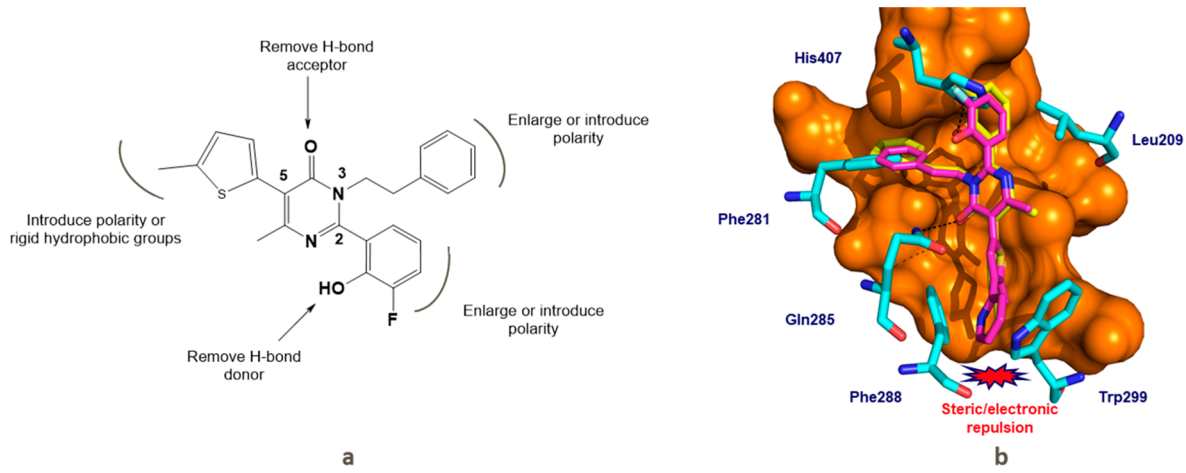

Figure 6. (a) Pharmacophore-model-informed SAR strategy. (b) Docked structure of compound **8** (magenta) supporting elimination of PXR affinity (overlaid with the docked structure of compound **1** in yellow).

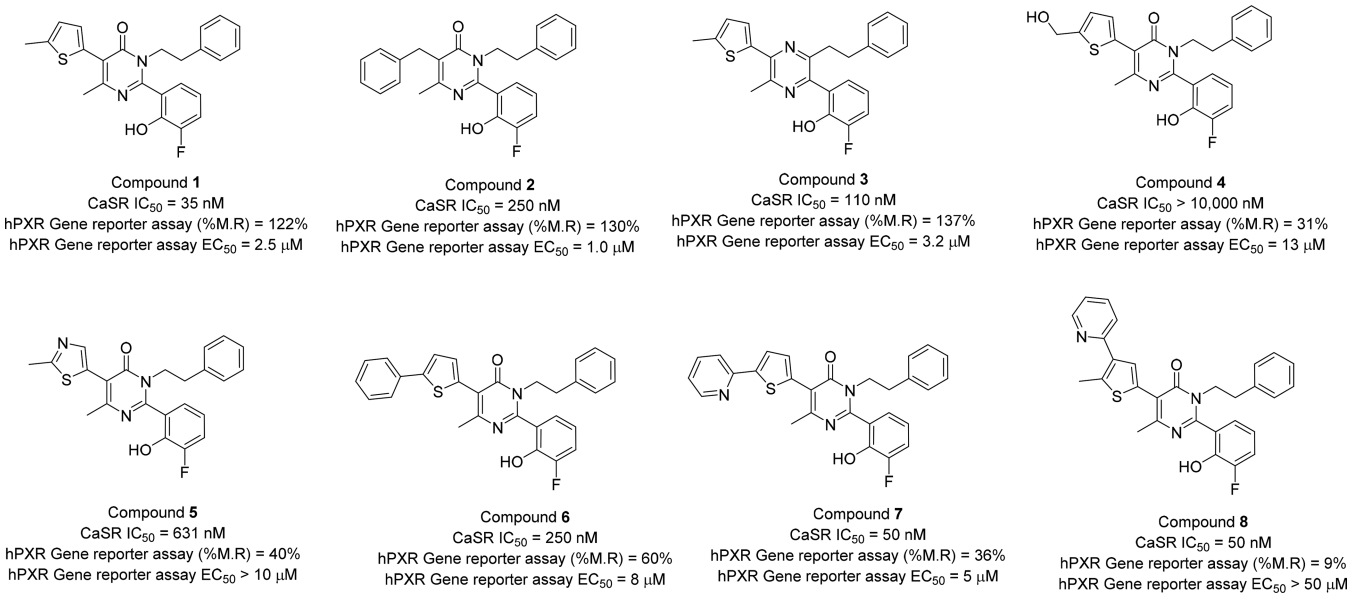

Figure 7. Structures and in vitro data of pyrimidinone-based CaSR antagonists **1**–**8**.

Table 2. Rat Toxicokinetic Parameters of Compounds 1 and 8 (Results Are Reported as Mean (n = 3) and [Range])

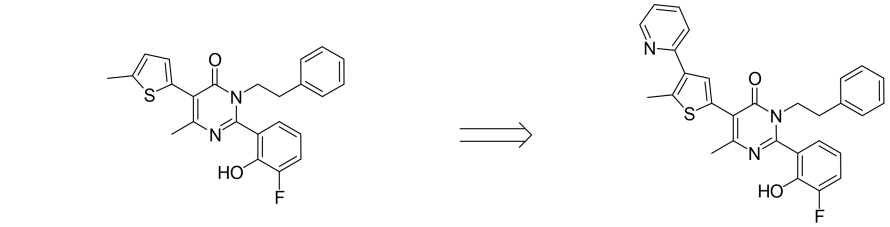

		AUC_{0-t} (μg h/mL)			C_{max} (μg/mL)		
compound	dose (mg kg^{-1} day^{-1})	day 1	day 10	fold diff.	day 1	day 10	fold diff.
1	300	2.5 [1.3–4.7]	1.8 [1.0–2.5]	−1.4	0.33	0.36	+1.1
8	100	29.5 [22.6–34.8]	41.1 [20.4–77.0]	+1.4	8.9	12	+1.3

neutral, and flexible demonstrated a high propensity to activate PXR. Contrarily, no single chemical property (molecular weight (MW), number of H-bond donors, number of H-bond acceptors, cLogD, number of ionizable groups) that abolishes

https://doi.org/10.1021/acsmedchemlett.1c00187
ACS Med. Chem. Lett. XXXX, XXX, XXX−XXX

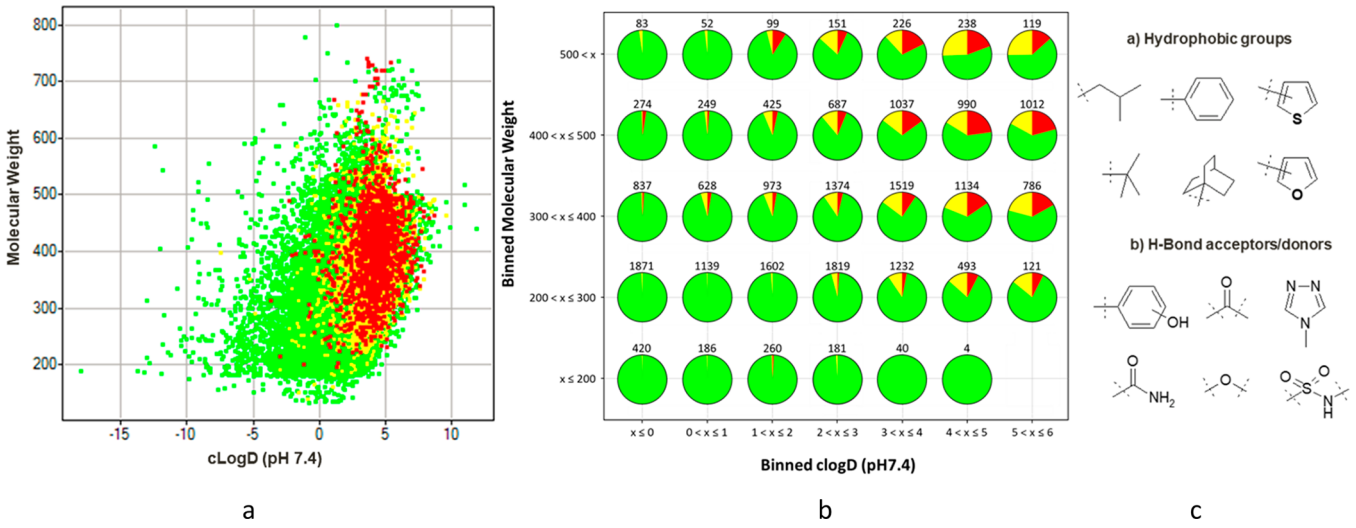

Figure 8. (a) Plots of MW and cLogD (pH 7.4) for compounds from the GSK compound collection. (b) Binning of MW and cLogD (pH 7.4) for the GSK compounds. Color coding reflects PXR activity (% maximum response), with red, yellow, and green corresponding to >70% (high), 30−70% (medium), and <30% (low) induction relative to 10 μM rifampicin, respectively (SI pp S8 and S9). (c) Exemplary functional groups observed as PXR activators.

PXR activity emerged. However, lower lipophilicity (cLogD < 2.5) and low MW displayed the strongest correlations (Figure 8). Additionally, not all CYP3A4 substrates are PXR inducers (data not shown). Since no clear trends to abolish PXR activity are available, the pharmacophore model that allows a priori prediction of PXR activation should greatly aid in compound design.

PXR activation is a primary reason for CYP3A4-induced drug−drug interactions and leads to attrition of preclinical and clinical assets.[27] Because of its indiscriminatory binding pocket, PXR accommodates a wide range of chemical classes commonly encountered in lead optimization. High levels of PXR induction by the pyrimidinone class of CaSR antagonists prompted us to investigate a rational way to abolish PXR-mediated CYP induction. Multiple conformations observed with SR12813 have injected uncertainty into cocrystal structure interpretations and subsequent pharmacophore models derived from them. The pharmacophore models reported to date were insufficient to rationalize the SAR trends for the PXR activity observed for the pyrimidinones.[28−30] Furthermore, in silico models reported to date were unable to emphasize the critical nature of specific interactions observed.[14−16,31] For instance, H-bonding to Gln285 was reported to be indispensable, and hydrophobic contacts are not essential for receptor activation. The above annotations have led to the development of a comprehensive model derived from diverse chemical classes. Our PXR model, unlike earlier models, emphasizes one key binding model for focused SAR investigations to overcome PXR affinity: incorporation of polar and/or rigid hydrophobic moieties at the bottom pocket featuring Phe288 and Trp299. A recent report provides evidence that Trp299 is a critical residue for binding and transactivation.[32] Elimination of H-bond-acceptor properties to remove the molecule anchoring ability may diminish binding but are not enough as claimed by the previous reports. Utilization of our pharmacophore model has led to a focused yet rapid SAR campaign on the pyrimidinone scaffold that produced several analogues devoid of PXR affinity. A full report detailing SAR investigations as well as drug metabolism, pharmacokinetic, pharmacodynamic, and safety data will be the subject of a future publication. In this paper, we have highlighted the ambiguity associated with PXR activation in pharmacophore models and SARs, thus fulfilling the need for the development of pharmacophore model with wider applicability.

■ ASSOCIATED CONTENT

Supporting Information

The Supporting Information is available free of charge at https://pubs.acs.org/doi/10.1021/acsmedchemlett.1c00187.

Experimental procedures; molecular modeling protocols; conditions and protocols for biological assays; interpretation of PXR activation; crystallography experimental methods, data, and structures; development of the pharmacophore model; and profile of compounds (PDF)

■ AUTHOR INFORMATION

Corresponding Author

Joshi M. Ramanjulu − *GlaxoSmithKline, Collegeville, Pennsylvania 19426, United States;* orcid.org/0000-0003-3471-651X; Phone: (484) 574-2304; Email: Joshi.M.Ramanjulu@gsk.com

Authors

Shawn P. Williams − *GlaxoSmithKline, Collegeville, Pennsylvania 19426, United States*

Ami S. Lakdawala − *GlaxoSmithKline, Collegeville, Pennsylvania 19426, United States*

Michael P. DeMartino − *GlaxoSmithKline, Collegeville, Pennsylvania 19426, United States*

Yunfeng Lan − *GlaxoSmithKline, Collegeville, Pennsylvania 19426, United States*

Robert W. Marquis − *GlaxoSmithKline, Collegeville, Pennsylvania 19426, United States*

Complete contact information is available at: https://pubs.acs.org/10.1021/acsmedchemlett.1c00187

https://doi.org/10.1021/acsmedchemlett.1c00187
ACS Med. Chem. Lett. XXXX, XXX, XXX−XXX

Author Contributions

A.S.L. conducted computational modeling, generation of the pharmacophore model, and molecular docking. S.P.W. performed X-ray analysis of the crystals. Y.L. and M.P.D. conducted the synthesis of pyrimidinone derivatives and interpreted the data for characterization of the compounds. J.M.R. oversaw PXR screening, supervised SAR studies, developed the concept, and wrote the manuscript. R.W.M. contributed to the program strategy. All of the authors approved the final version of the manuscript.

Notes

The authors declare no competing financial interest.

■ ACKNOWLEDGMENTS

The authors acknowledge Dr. Iain McLay, Group Leader (retired from GSK), for performing initial computational analysis of in-house crystal structures; Yingtao Lu, Xiaoyang Dong, and Robert Trout for preparation of compounds **2**, **3**, and **4**, respectively; Andrew Brown and Metul Patel for PXR assay writeup and data generation; Mark Mellinger for generation of analytical data; Tim Hart for providing safety assessment data; and Grazyna-Graczyk Millbrandt for the interpretation of NMR spectra.

■ ABBREVIATIONS

PXR, pregnane X receptor; DBD, DNA-binding domain; LBD, ligand-binding domain; NR, nuclear receptor; M.R, maximum response; CaSR, calcium sensing receptor; SAR, structure–activity relationship; PTH, parathyroid hormone; DDI, drug–drug interaction

■ REFERENCES

(1) Juurlink, D.; Mamdani, M.; Kopp, A.; Laupacis, A.; Redelmeier, D. Drug–Drug interactions among elderly hospitalized patients. *JAMA* **2003**, *289*, 1652–1658.

(2) Goodwin, B.; Redinbo, M. R.; Kliewer, S. A. Regulation of cyp3a gene transcription by the pregnane X receptor. *Annu. Rev. Pharmacol. Toxicol.* **2002**, *42*, 1–23.

(3) Handschin, C.; Meyer, U. A. Induction of Drug Metabolism: The Role of Nuclear Receptors. *Pharmacol. Rev.* **2003**, *55*, 649–673.

(4) Jones, S. A.; Moore, L. B.; Shenk, J. L.; Wisely, G. B.; Hamilton, G. A.; McKee, D. D.; Tomkinson, N. C.; LeCluyse, E. L.; Lambert, M. H.; Willson, T. M.; Kliewer, S. A.; Moore, J. T. The pregnane X receptor: a promiscuous xenobiotic receptor that has diverged during evolution. *Mol. Endocrinol.* **2000**, *14*, 27–39.

(5) Kliewer, S. A.; Willson, T. M. Regulation of xenobiotic and bile acid metabolism by the nuclear pregnane X receptor. *J. Lipid Res.* **2002**, *43*, 359–364.

(6) Kliewer, S. A.; Goodwin, B.; Willson, T. M. The nuclear pregnane X receptor: a key regulator of xenobiotic metabolism. *Endocr. Rev.* **2002**, *23*, 687–702.

(7) Kliewer, S. A.; Moore, J. T.; Wade, L.; Staudinger, J. L.; Watson, M. A.; Jones, S. A.; McKee, D. D.; Oliver, B. B.; Willson, T. M.; Zetterstrom, R. H.; Perlmann, T.; Lehmann, J. M. An orphan nuclear receptor activated by pregnanes defines a novel steroid signaling pathway. *Cell* **1998**, *92*, 73–82.

(8) Lin, J. H.; Lu, A. Y. Inhibition and Induction of P450 and the clinical Implications. *Clin. Pharmacokinet.* **1998**, *35* (5), 361–390.

(9) Oladimeji, P. O.; Chen, T. PXR: More Than Just a Master Xenobiotic Receptor. *Mol. Pharmacol.* **2018**, *93*, 119–127.

(10) Frank, C.; Makkonen, H.; Dunlop, T. W.; Matilainen, M.; Vaisanen, S.; Carlberg, C. Identification of pregnane X receptor binding sites in the regulatory regions of genes involved in bile acid homeostasis. *J. Mol. Biol.* **2005**, *346*, 505–519.

(11) Pavek, P. Pregnane X Receptor (PXR)-Mediated Gene Repression and Crosstalk of PXR with Other Nuclear Receptors via Coactivator Interactions. *Front. Pharmacol.* **2016**, *7*, 456.

(12) Watkins, R. E.; Wisely, G. B.; Moore, L. B.; Collins, J. L.; Lambert, M. H.; Williams, S. P.; Willson, T. M.; Kliewer, S. A.; Redinbo, M. R. The human nuclear xenobiotic receptor PXR: structural determinants of directed promiscuity. *Science* **2001**, *292*, 2329–2333.

(13) Xue, Y.; Chao, E.; Zuercher, W. J.; Willson, T. W.; Collins, J. L.; Redinbo, M. R. Crystal structure of the PXR–T1317 complex provides a scaffold to examine the potential for receptor antagonism. *Bioorg. Med. Chem.* **2007**, *15*, 2156–2166. Bartolini, D.; De Franco, F.; Torquato, P.; Marinelli, R.; Cerra, B.; Ronchetti, R.; Schon, A.; Fallarino, F.; De Luca, A.; Bellezza, G.; Ferri, I.; Sidoni, A.; Walton, W. G.; Pellock, S. J.; Redinbo, M. R.; Mani, S.; Pellicciari, R.; Gioiello, A.; Galli, F. Garcinoic Acid Is a Natural and Selective Agonist of Pregnane X Receptor. *J. Med. Chem.* **2020**, *63*, 3701–3712.

(14) Gao, Y.-D.; Olson, S. H.; Balkovec, J. M.; Zhu, Y.; Royo, I.; Yabut, J.; Evers, R.; Tan, E. Y.; Tang, W.; Hartley, D. P.; Mosley, R. T. Attenuating pregnane X receptor (PXR) activation: A molecular modelling approach. *Xenobiotica* **2007**, *37*, 124–138.

(15) Ekins, S.; Kortagere, S.; Iyer, M.; Reschly, E.; Lill, M. A.; Redinbo, M. R.; Krasowski, M. D. Challenges Predicting Ligand–Receptor Interactions of Promiscuous Proteins: The Nuclear Receptor PXR. *PLoS Comput. Biol.* **2009**, *5*, e1000594.

(16) Kortagere, S.; Krasowski, M. D.; Ekins, S. Ligand- and structure-based pregnane X receptor models. *Methods Mol. Biol.* **2012**, *929*, 359–375.

(17) Hannan, E. M.; Kallay, E.; Chang, W.; Brandi, M. L.; Thakker, R. V. The calcium-sensing receptor in physiology and in calcitropic and noncalcitropic diseases. *Nat. Rev. Endocrinol.* **2019**, *15*, 33–52.

(18) After administration of ketoconazole, the dose-normalized $AUC_{0-\infty}$ of compound **1** increased an average of 3.9-fold, and the dose-normalized C_{max} increased an average of 2.1-fold. Compound **1** is a substrate of 3A4. It is not a P-glycoprotein (P-gp) substrate. Ketoconazole is a dual inhibitor/modulator of human CYP3A/P-gp that is expressed extensively in the gut and liver. Ketoconazole had been shown to increase absorption and decrease first-pass metabolism of some CYP3A/P-gp substrates (e.g., erythromycin) in the monkey. The data from this study confirmed that **1** is a substrate of CYP3A.

(19) Luo, G.; Cunningham, M.; Kim, S.; Burn, T.; Lin, J.; Sinz, M.; Hamilton, G.; Rizzo, C.; Jolley, S.; Gilbert, D.; Downey, A.; Mudra, D.; Graham, R.; Carroll, K.; Xie, J.; Madan, A.; Parkinson, A.; Christ, D.; Selling, B.; LeCluyse, E.; Gan, L. S. CYP3A4 Induction by Drugs: Correlation between a Pregnane X Receptor Reporter Gene Assay and CYP3A4 Expression in Human Hepatocytes. *Drug Metab. Dispos.* **2002**, *30*, 795–804.

(20) Halladay, J. S.; Wong, S.; Khojasteh, S. C.; Grepper, S. An 'all-inclusive' 96-well cytochrome P450 induction method: Measuring enzyme activity, mRNA levels, protein levels, and cytotoxicity from one well using cryopreserved human hepatocytes. *J. Pharmacol. Toxicol. Methods* **2012**, *66*, 270–275.

(21) Casillas, L. N.; Charnley, A. K.; Harris, P. A.; Jeong, J. U.; Marquis, R. W.; Ramanjulu, J. M.; Trout, R. Preparation of 5-thienyl-4(3*H*) pyrimidinone derivatives as calcium receptor antagonists. WO 2010065383 A1, 2010.

(22) Casillas, L. N.; Charnley, A. K.; DeMartino, M. P.; Dong, X.; Harris, P. A.; Marquis, R. W.; Ramanjulu, J. M.; Trout, R. Preparation of thienyl pyrimidinone compounds as calcilytic agents for treating diseases associated with abnormal bone or mineral homeostasis. WO 2010039922 A1, 2010.

(23) Ramanjulu, J. M.; DeMartino, M.; Lan, Y.; Marquis, R. Titanium isopropoxide mediated synthesis of pyrimidin-4-ones. *Org. Lett.* **2010**, *12*, 2270–2273.

(24) Jeong, J.; Ramanjulu, J. M.; Marquis, R. W. Preparation of pyrazine derivatives as calcium receptor antagonists. WO 2009006245 A2, 2009.

(25) Voss, N. R.; Gerstein, M. 3V: cavity, channel and cleft volume calculator and extractor. *Nucleic Acids Res.* **2010**, *38*, W555–W562.

https://doi.org/10.1021/acsmedchemlett.1c00187
ACS Med. Chem. Lett. XXXX, XXX, XXX–XXX

(26) McMartin, C.; Bohacek, R. S. QXP: Powerful, Rapid Computer Algorithms for Structure-Based Drug Design. *J. Comput.-Aided Mol. Des.* **1997**, *11*, 333−344.
(27) Shukla, S. J.; Sakamuru, S.; Huang, R.; Moeller, T. A.; Shinn, P.; VanLeer, D.; Auld, D. S.; Austin, C. A.; Xia, M. Identification of Clinically Used Drugs That Activate Pregnane X Receptors. *Drug Metab. Dispos.* **2011**, *39*, 151−159.
(28) Masuyama, H.; Suwaki, N.; Tateishi, Y.; Nakatsukasa, H.; Segawa, T.; Hiramatsu, Y. The pregnane X receptor regulates gene expression in a ligand- and promoter-selective fashion. *Mol. Endocrinol.* **2005**, *19*, 1170−80.
(29) Vaz, R. J.; Li, Y.; Chellaraj, V.; Reiling, S.; Kuntzweiler, T.; Yang, D.; Shen, H.; Batchelor, J. D.; Zhang, Y.; Chen, X.; McLean, L. R.; Kosley, R., Jr. Amelioration of PXR-mediated CYP3A4 induction by mGluR2 modulators. *Bioorg. Med. Chem. Lett.* **2018**, *28*, 3194−3196.
(30) Wu, B. J.; Li, S.; Dong, D. 3D structures and ligand specificities of nuclear xenobiotic receptors CAR, PXR and VDR. *Drug Discovery Today* **2013**, *18*, 574−581.
(31) Torimoto-Katori, N.; Huang, R.; Kato, H.; Ohashi, R.; Xia, M. *In Silico* Prediction of hPXR Activators Using Structure-Based Pharmacophore Modeling. *J. Pharm. Sci.* **2017**, *106*, 1752−1759.
(32) Banerjee, M.; Chai, S. C.; Wu, J.; Robbins, D.; Chen, T. Tryptophan 299 is a conserved residue of human pregnane X receptor critical for the functional consequence of ligand binding. *Biochem. Pharmacol.* **2016**, *104*, 131−138.

https://doi.org/10.1021/acsmedchemlett.1c00187
ACS Med. Chem. Lett. XXXX, XXX, XXX−XXX